

# Absorption spectrum of phytoplankton pigments derived from hyperspectral remote-sensing reflectance

ZhongPing Lee<sup>a,\*</sup>, Kendall L. Carder<sup>b</sup>

<sup>a</sup>Stennis Space Center, MS, Naval Research Lab., Code 7333 39529, USA

<sup>b</sup>College of Marine Science, University of South Florida, St. Petersburg, FL 33701, USA

Received 22 August 2003; received in revised form 21 October 2003; accepted 23 October 2003

## Abstract

For a data set collected around Baja California with chlorophyll-*a* concentration ((chl-*a*)) ranging from 0.16 to 11.3 mg/m<sup>3</sup>, hyperspectral absorption spectra of phytoplankton pigments were independently inverted from hyperspectral remote-sensing reflectance using a newly developed ocean-color algorithm. The derived spectra were then compared with those measured from water samples using the filter-pad technique, and an average difference of 21.4% was obtained. These results demonstrate that the inversion algorithm worked quite well for the coastal waters observed and suggest a potential of using hyperspectral remote sensing to retrieve both chlorophyll-*a* and other accessory pigments.

© 2003 Elsevier Inc. All rights reserved.

**Keywords:** Absorption spectrum of phytoplankton pigments; Inversion algorithms

## 1. Introduction

Absorption of phytoplankton play important roles in modulating subsurface light field and contributing to photosynthesis (Gordon et al., 1988; Morel, 1988; Platt & Sathyendranath, 1988). Decades of field study have found that the spectra of phytoplankton absorption ( $a_{\phi}(\lambda)$ ) vary in both magnitude and spectral shape (Ciotti, Lewis, & Cullen, 2002; Hoepffner & Sathyendranath, 1991; Kirk, 1986; Sathyendranath, Lazzara, & Prieur, 1987), with the difference an indication of different pigment compositions (Bidigare, Ondrusek, Morrow, & Kiefer, 1990; Hoepffner & Sathyendranath, 1991; Sathyendranath et al., 1987) or cell sizes (Ciotti et al., 2002). Hoepffner and Sathyendranath (1993) demonstrated that pigment compositions can be derived from a hyperspectral  $a_{\phi}(\lambda)$  spectrum after applying a series of Gaussian bands reflecting absorption by phytoplankton pigments (Hoepffner & Sathyendranath, 1993); Ciotti et al. (2002) indicated that phytoplankton cell size can be implied from hyperspectral  $a_{\phi}(\lambda)$ ; Cullen, Davis, and Lewis (1997) suggested using phytoplankton absorption to detect harmful algal blooms; and Millie et al. (1997) used

$a_{\phi}(\lambda)$  to analyze the abundance of *Gymnodinium breve* (red tide dinoflagellate). All these analyses require that hyperspectral  $a_{\phi}(\lambda)$  spectra be inputted, as measured by the filter-pad transmission techniques after water samples are collected (Bricaud & Stramski, 1990; Mitchell & Kiefer, 1988; Mueller & Fargion, 2002). This measurement approach, however, can only be applied to discrete water samples, impractical for measurements over large areas.

Water color can be effectively measured over broad regions using satellite sensors, and it has been demonstrated that chlorophyll-*a* concentrations ((chl-*a*)) can be derived from the measurements of water color (Gordon et al., 1983; Morel & Prieur, 1977). Current ocean-color remote sensing, limited by algorithms and sensor configurations, are mainly focused on the retrieval of (chl-*a*) (Carder, Chen, Lee, Hawes, & Kamykowski, 1999; Doerffer & Fisher, 1994; Morel & Gentili, 1996; O'Reilly et al., 1998). Since information on accessory pigments can help the differentiation into major phytoplankton classes or taxonomic groups (Hoepffner & Sathyendranath, 1993), it would be a great enhancement to ocean-color remote sensing if information regarding accessory pigments can also be retrieved from water color. For this purpose, one approach is to retrieve  $a_{\phi}(\lambda)$  spectra from ocean-color remote sensing.

Most existing methods (Bukata, Jerome, Bruton, Jain, & Zwick, 1981; Doerffer & Fisher, 1994; Garver & Siegel,

\* Corresponding author. Tel.: +1-228-688-4873.

E-mail address: [zplee@nrlssc.navy.mil](mailto:zplee@nrlssc.navy.mil) (Z.P. Lee).

1997; Hoge & Lyon, 1996; Lee, Carder, Peacock, Davis, & Mueller, 1996; Maritorena, Siegel, & Peterson, 2000; Roesler & Perry, 1995) in ocean-color inversion require a prior knowledge of the spectral shape of  $a_{\phi}(\lambda)$ . These inversion methods, though, working well in deriving the major properties such as the chlorophyll-*a* concentrations, prevent the independent derivation of  $a_{\phi}(\lambda)$  spectra since its spectral dependence is assumed known already and is used during the retrieval process. Actually, the spectral dependence of  $a_{\phi}(\lambda)$  is a property to be derived from remotely sensed data. Also, incorrect assumptions regarding  $a_{\phi}(\lambda)$  shape will lead to errors in retrieved properties.

The quasi-analytical algorithm (QAA) recently developed by Lee, Carder, and Arnone (2002) does not need a hyperspectral  $a_{\phi}(\lambda)$  spectrum in the ocean-color inversion process. The algorithm was tested with multi-band, computer-simulated data and found that  $a_{\phi}(\lambda)$  retrieved from remote sensing were within  $\sim 15\%$  of the input values (Lee et al., 2002). For the derivation of  $a_{\phi}(\lambda)$  spectra, however, it is not known how well QAA performs with field collected hyperspectral data.

In this study, QAA is applied to a data set collected from waters around Baja California, which bears no relation to the data set used in algorithm development (Lee et al., 2002). Using measured hyperspectral remote-sensing reflectance as input, the absorption spectra of phytoplankton pigments were analytically calculated. The derived spectra were then compared with those measured from water samples using the filter-pad technique. The study here intends to test the performance of the algorithm using an independent data set from field measurements, and to look at the potential to independently retrieve  $a_{\phi}(\lambda)$  spectra from hyperspectral remote sensing.

## 2. Data and measurement methods

Field data collected in October 1999 around Baja California during the Marine Optical Characterization Experiment 5 (MOCE5) were used in this study. Fig. 1 indicates the locations of the 20 stations where measurements were made, with the number in the parenthesis for the measured attenuation coefficient at 490 nm ( $K_d(490)$ ). For each station, remote-sensing reflectance was measured using a handheld spectroradiometer, while phytoplankton pigment absorption coefficients were measured from collected water samples using the GF/F filter-pad transmission technique (Bricaud & Stramski, 1990; Mitchell & Kiefer, 1988).

### 2.1. Above-surface remote-sensing reflectance, $R_{rs}(\lambda)$

Above-surface remote-sensing reflectance ( $R_{rs}$ ) is defined as the ratio of the water-leaving radiance to the downwelling irradiance just above the surface. As water-leaving radiance cannot be directly measured from above

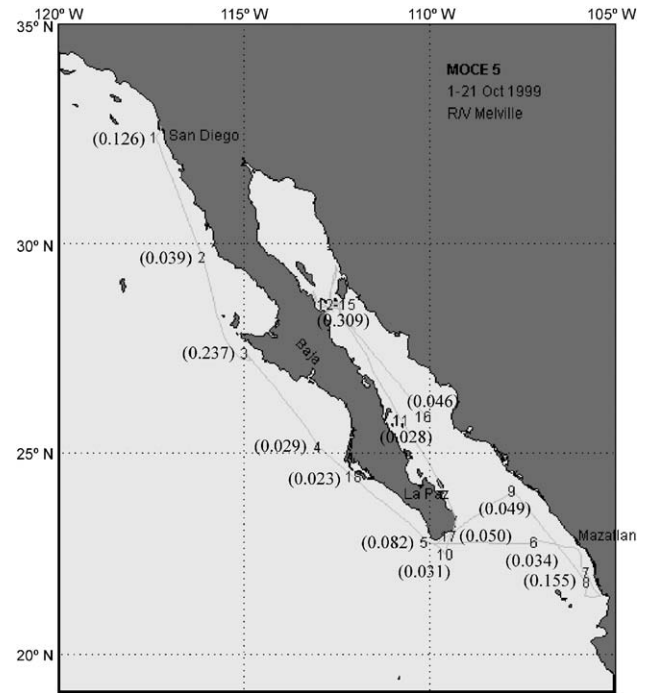


Fig. 1. Locations of data collected in this study. Values in parenthesis are the attenuation coefficient at 490 nm of that station.

the surface,  $R_{rs}$  was determined by correcting for the surface-reflected skylight and solar glint from the measured upwelling radiance, using a method (Lee, Carder, Steward et al., 1996) extending the approach described in Carder and Steward (1985).

Briefly, multiple spectra of above-surface upwelling radiance ( $L_u$ ) and downwelling sky radiance ( $L_{sky}$ ) were collected during daylight stations from the bow of the ship to avoid ship shadow and wake bubbles.  $L_u$  was measured at  $30^\circ$  from nadir and  $L_{sky}$  was measured at  $30^\circ$  from zenith, both in a plane  $90^\circ$  to the solar plane. The instrument used was a custom-made, hand-held 512-channel spectroradiometer with wavelengths ranging from 360 to 890 nm, and it was equipped with a  $10^\circ$  field stop. The water-leaving radiance was then calculated by subtracting from the total upwelled radiance the portion of the skylight reflected into the sensor along with any solar glint (Lee, Carder, Steward et al., 1996):

$$L_w = L_u - r(i) \times L_{sky}(i) - \Delta E_d, \quad (1)$$

where  $r(i) = 0.022$ , which is the Fresnel reflectance for the zenith angle ( $i$ ) at  $30^\circ$ . For open ocean waters,  $\Delta E_d$ , a solar glint correction, is estimated by assuming  $L_w(750) = 0$ . For coastal waters,  $\Delta E_d$  is estimated iteratively (Lee, Carder, Steward et al., 1996) without assuming  $L_w(750) = 0$ .

Using the measured radiance ( $L_G$ ) normal to a standard diffuse reflectance panel (Spectralon), the total downwelling irradiance ( $E_d$ ) is determined by  $E_d = \pi L_G / R_G$ , where  $R_G$  is the reflectance of the diffuse panel ( $\sim 10\%$ ). Then,  $R_{rs} =$

$L_w/E_d$ . In the process of calculating  $L_w$ , the averaged spectra of  $L_u$  and  $L_{sky}$  were used (Lee, Carder, Steward et al., 1996) after discarding any obvious outliers.

## 2.2. Phytoplankton pigment absorption coefficient, $a_\phi(\lambda)$

Phytoplankton pigment absorption coefficient ( $a_\phi$ ) was measured following the SeaWiFS protocols (Mueller & Fargion, 2002). Basically, surface water samples collected with an 8-l Niskin bottle were immediately filtered under low pressure through 2.5 cm GF/F filters. The volume of water filtered varied between  $\sim 0.2$  and 6.0 l depending on the concentration of particles in the sample. The method described in Mitchell and Kiefer (1988) was used to measure the particle absorption coefficients ( $a_p$ ), and the method developed by Kishino, Takahashi, Okami, and Ichimura (1985) and modified by Roesler, Perry, and Carder (1989) was used to measure the detritus absorption ( $a_d$ ) in order to calculate the pigment absorption coefficient ( $a_\phi$ ). In the calculations of  $a_p$  and  $a_d$ , the “ $\beta$  factor” from Carder et al. (1999), which is an average of two published formulations

(Bricaud & Stramski, 1990; Nelson & Robertson, 1993), was used for the correction of the optical-path elongation due to filter-pad multiple scattering. The difference between  $a_p(\lambda)$  and  $a_d(\lambda)$  provided  $a_\phi(\lambda)$ . The final  $a_\phi(\lambda)$  spectra were obtained by adjusting the calculated spectra until  $a_\phi(780) = 0$ .

## 3. Inversion methods

The Lee et al. (2002) QAA was used to derive the absorption spectrum of phytoplankton. Table 1 provides a shortened description of the inversion process (details of the algorithm can be found in Lee et al., 2002). Briefly, the total absorption spectra ( $a(\lambda)$ ) are first derived from the hyperspectral remote-sensing reflectance ( $R_{rs}(\lambda)$ ), after selecting a reference wavelength ( $\lambda_0$ , 555 or 640 nm) and applying a hyperbolic spectral model (Gordon & Morel, 1983) for the particle backscattering coefficient ( $bb_p(\lambda)$ ). Using the values of  $a(410)$  and  $a(440)$  with the estimated values of  $\zeta (= a_\phi(410)/a_\phi(440))$  and  $\xi (= a_g(410)/a_g(440))$ , the gelbstoff absorption coefficient at 440 nm ( $a_g(440)$ ) is calculated

Table 1  
Steps of deriving phytoplankton absorption spectrum from hyperspectral remote-sensing reflectance

Steps	Property	Derivation
Step 0	$r_{rs}$	$= R_{rs}/(0.52 + 1.7R_{rs})$
Step 1	$u(\lambda) = \frac{bb(\lambda)}{a(\lambda) + bb(\lambda)}$	$= \frac{-0.0895 + \sqrt{(0.0895)^2 + 4g_1r_{rs}(\lambda)}}{20.1247}$
Step 2	$a(\lambda_0)$ : $a(555)$ or $a(640)$	$a(555) = 0.0596 + 0.2(a(440)_i - 0.01)$ , $a(440)_i = \exp(-1.8 - 1.4\rho + 0.2\rho^2)$ , $\rho = \ln(r_{rs}(440)/r_{rs}(555))$
Step 3	$bb_p(\lambda_0)$	$= \frac{u(\lambda_0)a(\lambda_0)}{1 - u(\lambda_0)} - bb_w(\lambda_0)$
Step 4	$Y$	$= 2.2(1 - 1.2e^{-0.9r_{rs}(440)/r_{rs}(555)})$
Step 5	$bb_p(\lambda)$	$= bb_p(\lambda_0) \left(\frac{\lambda_0}{\lambda}\right)^Y$
Step 6	$a(\lambda)$	$= \frac{(1 - u(\lambda))(bb_w(\lambda) + bb_p(\lambda))}{u(\lambda)}$
Step 7	$\zeta = a_\phi(410)/a_\phi(440)$	$= 0.71 + \frac{0.06}{0.8 + r_{rs}(440)/r_{rs}(555)}$
Step 8	$\xi = a_g(410)/a_g(440)$	$= e^{-S(410 - 440)}$
Step 9	$a_g(440)$	$= \frac{(a(410) - \zeta a(440))}{\xi - \zeta} - \frac{(a_w(410) - \zeta a_w(440))}{\xi - \zeta}$
Step 10	$a_\phi(\lambda)$	$= a(\lambda) - a_g(440)e^{-S(\lambda - 440)} - a_w(\lambda)$

by solving a set of simple algebraic equations (Lee et al., 2002). Since  $a(\lambda)$  can be expressed as: (Carder et al., 1991; Gordon, Smith, & Zaneveld, 1980)

$$a(\lambda) = a_w(\lambda) + a_g(\lambda) + a_\phi(\lambda), \quad (2)$$

and  $a_g(\lambda)$  can be modeled as (Bricaud, Morel, & Prieur, 1981; Carder et al., 1991)

$$a_g(\lambda) = a_g(440)e^{-S(\lambda-440)}, \quad (3)$$

it is straightforward to calculate  $a_\phi(\lambda)$  after  $a(\lambda)$  and  $a_g(\lambda)$  are known:  $a_\phi(\lambda) = a(\lambda) - a_w(\lambda) - a_g(\lambda)$ . Here,  $a_w(\lambda)$  is the absorption spectrum of pure water, which was taken from Pope and Fry (1997).

The spectral slope  $S$  for  $a_g(\lambda)$ , which is a combination of both gelbstoff and phytoplankton detritus (Carder et al., 1991; Lee et al., 2002), can vary in a range from 0.01 to  $0.02 \text{ nm}^{-1}$  (Carder, Steward, Harvey, & Ortner, 1989; Kirk, 1994; Reynolds, Stramski, & Mitchell, 2001), and it is difficult to accurately estimate its value remotely. As in other coastal-water studies (Kirk, 1994; Lee et al., 2002; Lee, Carder, Chen, Peacock, 2001), an average  $S$  value of  $0.015 \text{ nm}^{-1}$  was used for all stations in this study.

#### 4. Results and discussion

The measured hyperspectral  $R_{rs}(\lambda)$  of the 20 stations are presented in Fig. 2. Though all 20 stations are not far from the coast lines (see Fig. 1), there were significant variations in magnitudes and spectral shapes among the measured  $R_{rs}(\lambda)$ , which clearly indicates that different types of waters exist in the region. This water-property variation is supported by the measurements taken from the water samples, as the measured chlorophyll-*a* concentration varied from  $1.98 \text{ mg/m}^3$  at Station 3 ( $K_d(490)$  was  $0.237 \text{ m}^{-1}$ ) to  $0.16$

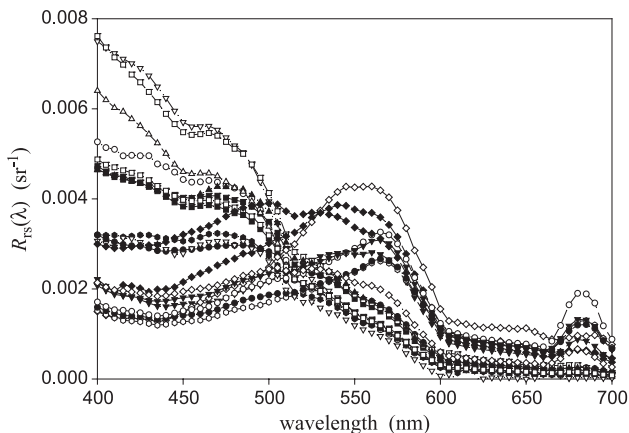


Fig. 2. Spectra of the measured remote-sensing reflectance of the 20 stations.

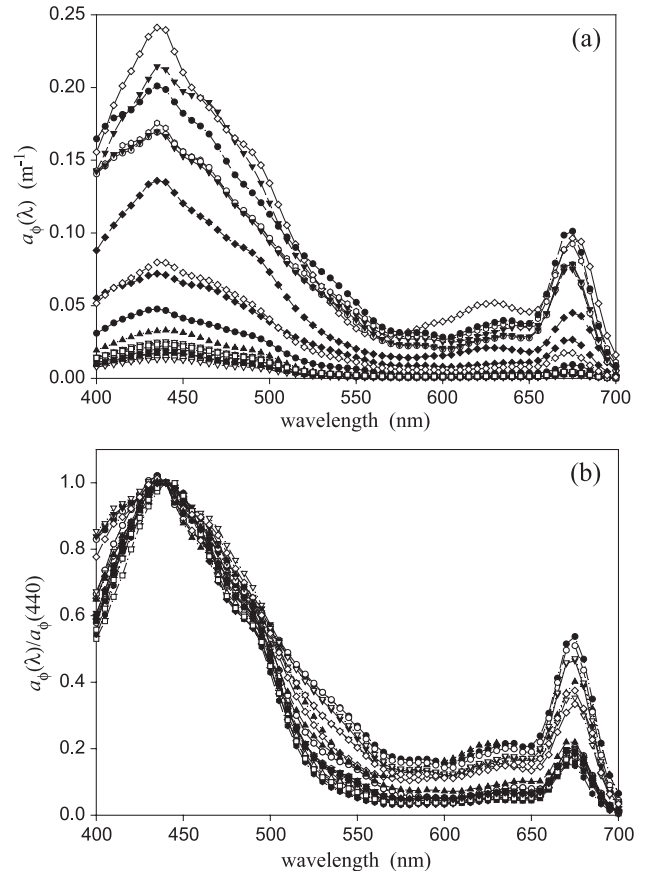


Fig. 3. Measured  $a_\phi(\lambda)$  spectra (a) and spectral curvature ( $a_\phi(\lambda)/a_\phi(440)$ ) (b) of the 20 stations.

$\text{mg/m}^3$  at the nearby Station 4 ( $K_d(490)$  was  $0.029 \text{ m}^{-1}$ ). Of the 20 coastal-water stations, the (chl-*a*) spanned a range of  $0.16$  to  $11.3 \text{ mg/m}^3$ , and  $K_d(490)$  varied from  $0.023$  to  $0.309 \text{ m}^{-1}$  (see Fig. 1), indicating strong local influence to the water properties.

Such wide variations were also found in the pad-measured  $a_\phi(\lambda)$  spectra (Fig. 3a and b), where  $a_\phi(440)$  varied from  $0.013$  to  $0.24 \text{ m}^{-1}$  among the 20 stations. The different  $a_\phi(\lambda)$  curvatures ( $a_\phi(\lambda)/a_\phi(440)$ , Fig. 3b) indicate that a single  $a_\phi(\lambda)$  spectral shape cannot be used in remote-sensing inversions for all stations, though all were in coastal waters of the same area. Of these samples, the ratio of  $a_d(440)/a_p(440)$  varied from  $0.03$  to  $0.14$ , suggesting more absorption from phytoplankton pigments than that from detritus materials.

In the derivation of  $a(\lambda)$  spectra from  $R_{rs}(\lambda)$ , the particle backscattering spectra ( $bb_p(\lambda)$ ) were derived first. For each spectrum, there are two model parameters:  $bb_p(\lambda_0)$  and  $Y$ .  $Y$  is a parameter describing the spectral variation of  $bb_p(\lambda)$  (Gordon & Morel, 1983), and is empirically derived from the measured reflectance (see Table 1).  $bb_p(\lambda_0)$  is derived from  $a(\lambda_0)$  and  $R_{rs}(\lambda_0)$ . The derived  $bb_p(\lambda)$  spectra (see Fig. 4) varied in both magnitudes and spectral shapes, as expected for different waters indicated by the measured reflectance. No error analyses involving  $bb_p(\lambda)$  were made,

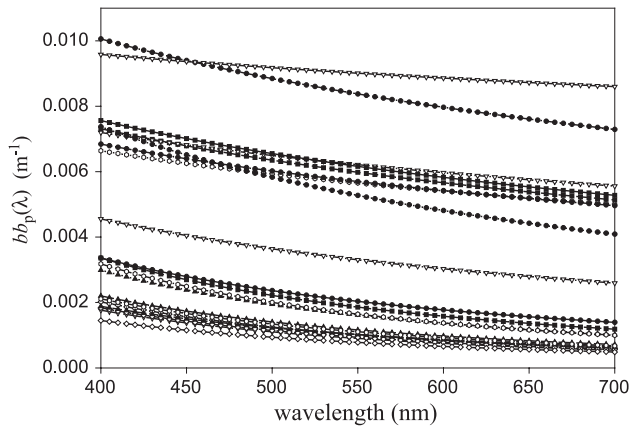


Fig. 4. Modeled particle backscattering spectra of the 20 stations. Model parameters of each station are derived from the measured remote-sensing reflectance (see Table 1).

as this was not the focus of this study and no hyperspectral data were available for such a comparison.

Fig. 5 presents the reflectance-derived  $a_{\phi}(\lambda)$  spectra of the 20 stations. No  $a_{\phi}(\lambda)$  were shown for wavelengths greater than 580 nm. This is due to the fact that for such wavelengths the total absorption coefficient is generally dominated by that of pure water.  $R_{rs}(\lambda)$  at those wavelengths provides limited or no information about  $a_{\phi}(\lambda)$ , so  $a_{\phi}(\lambda)$  cannot be directly and accurately derived from the  $R_{rs}(\lambda)$  at such wavelengths, except for eutrophic waters when  $a_{\phi}(\lambda)$  makes significant contributions to the total  $a(\lambda)$ . Of these derived  $a_{\phi}(\lambda)$  spectra, they show wide variations in magnitudes and spectral curvatures that are consistent with those from sample measurements.

These reflectance-derived  $a_{\phi}(\lambda)$  spectra were compared with those of water samples. Fig. 6 shows the comparison of a few selected wavelengths. In linear regression analysis, a slope of 0.921 with an intercept of  $-0.002 \text{ m}^{-1}$  were obtained ( $R^2 = 0.987$ ,  $N = 100$ ), with a percentage difference of 16.6%. These results suggest that the two sets of  $a_{\phi}(\lambda)$  values agree with each other very well.

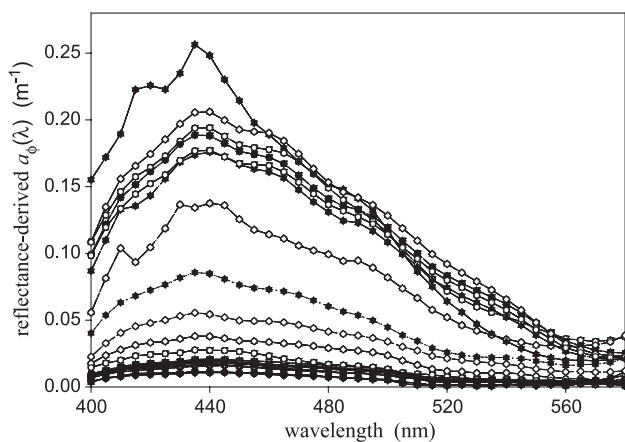


Fig. 5. Reflectance-derived  $a_{\phi}(\lambda)$  spectra of the 20 stations.

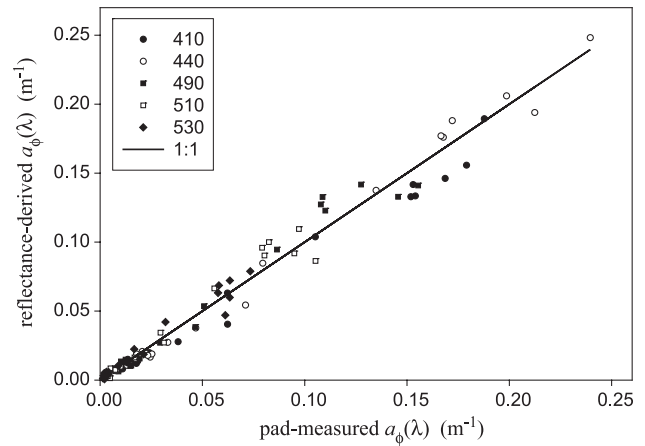


Fig. 6. Reflectance-derived  $a_{\phi}(\lambda)$  compared with pad-measured  $a_{\phi}(\lambda)$  at selected wavelengths.

To quantify the difference between the two  $a_{\phi}(\lambda)$  spectra for each station, the percentage difference (pd) between pad-measured spectrum ( $a_{\phi}(\lambda)_{\text{pad}}$ ) and reflectance-derived spectrum ( $a_{\phi}(\lambda)_{\text{der}}$ ) was calculated as follow,

$$\text{pd} = \frac{\sqrt{\text{mean}(a_{\phi}(\lambda)_{\text{pad}} - a_{\phi}(\lambda)_{\text{der}})^2}}{\text{mean}(a_{\phi}(\lambda)_{\text{pad}})} \times 100\%, \quad (4)$$

for a wavelength range of 400–580 nm. This wavelength range covers the broad  $a_{\phi}(\lambda)$  values around the blue peak, where  $a_{\phi}(\lambda)$  spectra vary the most.

For the 20 stations that measurements were made in this study, the pd values ranged from 8.8% to 38.3% with an average of 21.4%. Due to the nature of each method used, it is not clear yet what contribute most to the difference as neither pad- $a_{\phi}(\lambda)$  nor reflectance- $a_{\phi}(\lambda)$  can be considered error-free. For instance, there is 10–20% uncertainty in the pad-measured  $a_{\phi}(\lambda)$  values due to “ $\beta$  factor” used to correct the path-elongation effect (Bricaud, Morel, Babin, Allali, & Claustre, 1998; Carder et al., 1999; Mitchell & Kiefer, 1988). On the reflectance-derived  $a_{\phi}(\lambda)$  side, there were a couple of parameters and models used in the derivation process (see (Lee et al., 2002)), which are imperfect yet in ocean-color inversion. For example, a constant  $S$  value of  $0.015 \text{ nm}^{-1}$  was used for all stations even though the 20 stations actually covered different water types. Conceptually, different  $S$  values should be used for each station and more consistent  $a_{\phi}(\lambda)$  retrievals from reflectance could be expected. Unfortunately, it is not yet known how to accurately decide the  $S$  value based on information available from remote sensing. Note that errors in these parameters and models more or less will be propagated to the derived  $a_{\phi}(\lambda)$ .

We must also keep in mind that pad-measured  $a_{\phi}(\lambda)$  spectra are for discrete surface water samples while reflectance-derived  $a_{\phi}(\lambda)$  spectra are for the upper water column

(Gordon & Clark, 1980). Considering the combination of these uncertainties and errors, an average difference of 21.4% for wavelengths ranging from 400 to 580 nm is quite small and encouraging, indicating the  $a_{\phi}(\lambda)$  spectra derived from the two completely different methods were consistent with each other. This consistency indirectly validates the QAA algorithm used for the  $a_{\phi}(\lambda)$  derivation from hyperspectral  $R_{rs}(\lambda)$ , providing a potential to retrieve both major and minor pigments from hyperspectral remote sensing when combined with other modeling efforts (e.g., (Hoepffner & Sathyendranath, 1993)).

As examples, Fig. 7a (for Station 8) and Fig. 7b (for Station 11) show the best and worst  $a_{\phi}(\lambda)$  comparisons of this data set, with their  $R_{rs}(\lambda)$  also shown. Both Station 8 and Station 11 were near the mouth of California bay, but the (chl-*a*) was 3.76 mg/m<sup>3</sup> at Station 8 ( $K_d(490)$  was 0.155 m<sup>-1</sup>), and 0.32 mg/m<sup>3</sup> at Station 11 ( $K_d(490)$  was 0.028 m<sup>-1</sup>), with a 10-fold difference in the measured  $a_{\phi}(440)$ . These contrasts are also very distinctive in the measured  $R_{rs}(\lambda)$ .

For the reflectance-derived spectrum,  $a_{\phi}(\lambda)$  in the range of 400–580 nm were directly derived from the measured  $R_{rs}(\lambda)$  as described in Section 3, while  $a_{\phi}(\lambda)$  in the range of 580–700 nm were based on the model of Lee, Carder, Mobley, Steward, and Patch (1998), after a smooth connection around 580 nm. This extension to 700 nm is merely for direct and visual comparison with the pad-measured  $a_{\phi}(\lambda)$  as the latter was measured in the

range of 400–700 nm. In the  $a_{\phi}(\lambda)$  comparison, the two  $a_{\phi}(\lambda)$  spectra are nearly identical in values and curvature for Station 8, indicating a successful retrieval of  $a_{\phi}(\lambda)$  from  $R_{rs}(\lambda)$  and/or from water samples. At Station 11, however, the reflectance-derived  $a_{\phi}(\lambda)$  is about 30% smaller than the pad-measured  $a_{\phi}(\lambda)$ . Similar differences were also found when a spectral optimization method (Lee, Carder, Mobley, Steward, & Patch, 1999) was used. It is not clear yet what caused this bigger difference, and more studies are necessary to pinpoint the most likely reasons.

## 5. Summary

The QAA recently developed by Lee et al. (2002) is applied to a field-collected data set to test its potential of independently retrieving absorption spectra of phytoplankton pigments from hyperspectral remote sensing. The data set contains measured remote-sensing reflectance spectra ( $R_{rs}(\lambda)$ ) and phytoplankton absorption spectra ( $a_{\phi}(\lambda)$ ), taken from waters around Baja California, covering a (chl-*a*) range of 0.16–11.3 mg/m<sup>3</sup>.

By analytically inverting measured  $R_{rs}(\lambda)$  spectra,  $a_{\phi}(\lambda)$  spectra were derived. This derivation, unlike other existing methods, does not need a hyperspectral  $a_{\phi}(\lambda)$  model in the process. The derived  $a_{\phi}(\lambda)$  spectra were then compared with the pad-measured  $a_{\phi}(\lambda)$  spectra, and an average percentage difference of 21.4% was obtained for wavelengths ranged from 400 to 580 nm. It is not clear yet what major factor or factors contribute to the difference, though the difference is quite small by remote-sensing standards (Hooker, McClain, & Holmes, 1993). As hyperspectral  $a_{\phi}(\lambda)$  can be used for the derivation of pigment composition (Hoepffner & Sathyendranath, 1993), the results of this study suggest a potential to estimate not only chlorophyll-*a* but also other accessory pigments through hyperspectral remote sensing. This kind of information is important and useful as it may help scientists to reach a long-anticipated goal: to monitor the variation and succession of phytoplankton classes for large areas by remote sensing (IOCCG, 2000).

## Acknowledgements

Financial support was provided by the following contracts and grants: NASA through NAS5-97137 (KC), NAS5-31716 (KC), and NAG5-3446 (KC); the Office of Naval Research through N00014-96-I-5013 (KC), and N00014-97-0006 (KC); and the Naval Research Lab through the Hyperspectral Character of the Coastal Zone Program (0601153N). The authors are extremely grateful to Dennis Clark for conducting the cruise and the NASA MODIS Science Team for supporting the cruise, and Dr. Charles Trees for the measurement of chlorophyll-*a* concentrations.

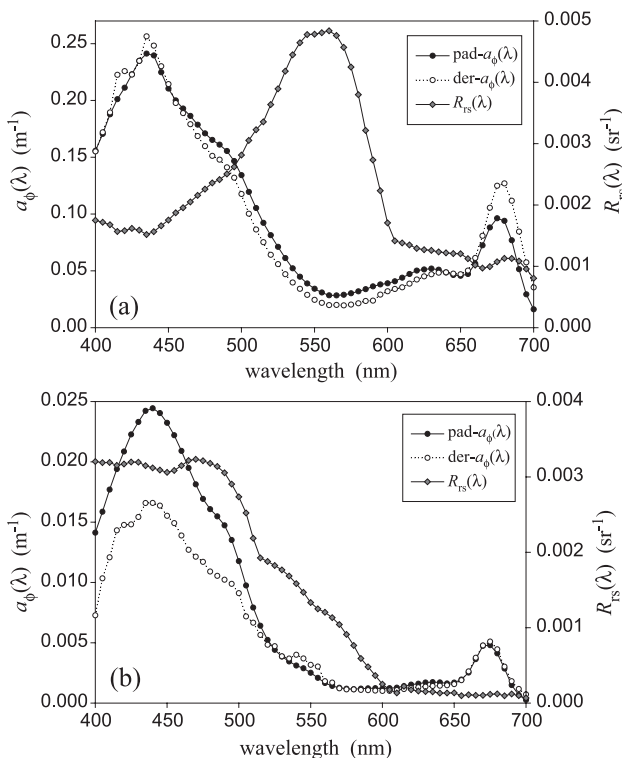


Fig. 7. The best and worst  $a_{\phi}(\lambda)$  comparison of this study, with (a) at Station 8 and (b) at Station 11.

The comments and suggestions from three anonymous reviewers are greatly appreciated.

## References

- Bidigare, R. R., Ondrusek, M. E., Morrow, J. H., & Kiefer, D. A. (1990). In vivo absorption properties of algal pigments. *Ocean Optics X, Proc. SPIE* (pp. 290–302).
- Bricaud, A., Morel, A., Babin, M., Allali, K., & Claustre, H. (1998). Variations of light absorption by suspended particles with chlorophyll *a* concentration in oceanic (case 1) waters: Analysis and implications for bio-optical models. *Journal of Geophysical Research*, *103*, 31033–31044.
- Bricaud, A., Morel, A., & Prieur, L. (1981). Absorption by dissolved organic matter of the sea (yellow substance) in the UV and visible domains. *Limnology and Oceanography*, *26*, 43–53.
- Bricaud, A., & Stramski, D. (1990). Spectral absorption coefficients of living phytoplankton and nonalgal biogenous matter: A comparison between the Peru upwelling area and the Sargasso Sea. *Limnology and Oceanography*, *35*, 562–582.
- Bukata, R. P., Jerome, J. H., Bruton, J. E., Jain, S. C., & Zwick, H. H. (1981). Optical water quality model of Lake Ontario: 2. Determination of chlorophyll *a* and suspended mineral concentration of natural waters from submersible and low altitude optical sensors. *Applied Optics*, *20*, 1704.
- Carder, K. L., Chen, F. R., Lee, Z. P., Hawes, S. K., & Kamykowski, D. (1999). Semianalytic moderate-resolution imaging spectrometer algorithms for chlorophyll-*a* and absorption with bio-optical domains based on nitrate-depletion temperatures. *Journal of Geophysical Research*, *104*, 5403–5421.
- Carder, K. L., Hawes, S. K., Baker, K. A., Smith, R. C., Steward, R. G., & Mitchell, B. G. (1991). Reflectance model for quantifying chlorophyll *a* in the presence of productivity degradation products. *Journal of Geophysical Research*, *96*, 20599–20611.
- Carder, K. L., & Steward, R. G. (1985). A remote-sensing reflectance model of a red tide dinoflagellate off West Florida. *Limnology and Oceanography*, *30*, 286–298.
- Carder, K. L., Steward, R. G., Harvey, G. R., & Ortner, P. B. (1989). Marine humic and fulvic acids: Their effects on remote sensing of ocean chlorophyll. *Limnology and Oceanography*, *34*, 68–81.
- Ciotti, A. M., Lewis, M. R., & Cullen, J. J. (2002). Assessment of the relationships between dominant cell size in natural phytoplankton communities and spectral shape of the absorption coefficient. *Limnology and Oceanography*, *47*, 404–417.
- Cullen, J. J., Ciotti, A. M., Davis, R. F., & Lewis, M. R. (1997). Optical detection and assessment of algal blooms. *Limnology and Oceanography*, *42*, 1223–1239.
- Doerffer, R., & Fisher, J. (1994). Concentrations of chlorophyll, suspended matter, and gelbstoff in case II waters derived from satellite coastal zone color scanner data with inverse modeling methods. *Journal of Geophysical Research*, *99*, 7466–7475.
- Garver, S. A., & Siegel, D. (1997). Inherent optical property inversion of ocean color spectra and its biogeochemical interpretation: 1. Time series from the Sargasso Sea. *Journal of Geophysical Research*, *102*, 18607–18625.
- Gordon, H. R., Brown, O. B., Evans, R. H., Brown, J. W., Smith, R. C., Baker, K. S., & Clark, D. K. (1988). A semianalytic radiance model of ocean color. *Journal of Geophysical Research*, *93*, 10909–10924.
- Gordon, H. R., & Clark, D. K. (1980). Remote sensing optical properties of a stratified ocean: An improved interpretation. *Applied Optics*, *19*, 3428–3430.
- Gordon, H. R., Clark, D. K., Brown, J. W., Brown, O. B., Evans, R. H., & Broenkow, W. W. (1983). Phytoplankton pigment concentrations in the Middle Atlantic Bight: Comparison of ship determinations and CZCS estimates. *Applied Optics*, *22*, 20–36.
- Gordon, H. R., & Morel, A. (1983). *Remote assessment of ocean color for interpretation of satellite visible imagery: A review*. New York: Springer (44 pp.).
- Gordon, H. R., Smith, R. C., & Zaneveld, J. R. V. (1980). Introduction to ocean optics. *Ocean Optics, vol. VI* (pp. 1–43). SPIE.
- Hoepffner, N., & Sathyendranath, S. (1991). Effect of pigment composition on absorption properties of phytoplankton. *Marine Ecology. Progress Series*, *73*, 11–23.
- Hoepffner, N., & Sathyendranath, S. (1993). Determination of the major groups of phytoplankton pigments from the absorption spectra of total particulate matter. *Journal of Geophysical Research*, *98*, 22789–22803.
- Hoge, F. E., & Lyon, P. E. (1996). Satellite retrieval of inherent optical properties by linear matrix inversion of oceanic radiance models: An analysis of model and radiance measurement errors. *Journal of Geophysical Research*, *101*, 16631–16648.
- Hooker, S. B., McClain, C. R., & Holmes, A. (1993). Ocean color imaging: CZCS to SeaWiFS. *Marine Technology Society Journal*, *27*, 3–15.
- IOCCG (2000). Remote sensing of ocean colour in coastal, and other optically-complex, waters. In S. Sathyendranath (Ed.), *Reports of the International Ocean-Colour Coordinating Group, vol. 3*. Dartmouth, Canada: IOCCG.
- Kirk, J. T. O. (1986). *Light and photosynthesis in aquatic ecosystems*. Cambridge: Cambridge Univ. Press.
- Kirk, J. T. O. (1994). *Light and photosynthesis in aquatic ecosystems*. Cambridge: University Press.
- Kishino, M., Takahashi, M., Okami, N., & Ichimura, S. (1985). Estimation of the spectral absorption coefficients of phytoplankton in a thermally stratified sea. *Bulletin of Marine Science*, *37*, 634–642.
- Lee, Z. P., Carder, K. L., & Arnone, R. (2002). Deriving inherent optical properties from water color: A multi-band quasi-analytical algorithm for optically deep waters. *Applied Optics*, *41*, 5755–5772.
- Lee, Z. P., Carder, K. L., Chen, R. F., & Peacock, T. G. (2001). Properties of the water column and bottom derived from AVIRIS data. *Journal of Geophysical Research*, *106*, 11639–11652.
- Lee, Z. P., Carder, K. L., Mobley, C. D., Steward, R. G., & Patch, J. S. (1998). Hyperspectral remote sensing for shallow waters: 1. A semi-analytical model. *Applied Optics*, *37*, 6329–6338.
- Lee, Z. P., Carder, K. L., Mobley, C. D., Steward, R. G., & Patch, J. S. (1999). Hyperspectral remote sensing for shallow waters: 2. Deriving bottom depths and water properties by optimization. *Applied Optics*, *38*, 3831–3843.
- Lee, Z. P., Carder, K. L., Peacock, T. G., Davis, C. O., & Mueller, J. L. (1996). Method to derive ocean absorption coefficients from remote-sensing reflectance. *Applied Optics*, *35*, 453–462.
- Lee, Z. P., Carder, K. L., Steward, R. G., Peacock, T. G., Davis, C. O., & Mueller, J. L. (1996). Remote-sensing reflectance and inherent optical properties of oceanic waters derived from above-water measurements. In S. G. Ackleso, & R. Frouin (Eds.), *Ocean Optics, vol. XIII* (pp. 160–166). SPIE.
- Maritena, S., Siegel, D. A., & Peterson, A. R. (2000). Optimization of a semianalytical ocean color model for global-scale applications. *Applied Optics*, *41*, 2705–2714.
- Millie, D. F., Schofield, O. M., Kirkpatrick, G. J., Johnsen, G., Tester, P. A., & Vinyard, B. T. (1997). Detection of harmful algal blooms using photopigments and absorption signature: A case study of the Florida red tide dinoflagellate, *Gymnodinium breve*. *Limnology and Oceanography*, *42*, 1240–1251.
- Mitchell, B. G., & Kiefer, D. A. (1988). Chl-*a* specific absorption and fluorescence excitation spectra for light limited phytoplankton. *Deep-Sea Research*, *35*, 635–663.
- Morel, A. (1988). Optical modeling of the upper ocean in relation to its biogenous matter content (Case I waters). *Journal of Geophysical Research*, *93*, 10749–10768.
- Morel, A., & Gentili, B. (1996). Diffuse reflectance of oceanic waters: III. Implications of bi-directionality for the remote sensing problem. *Applied Optics*, *35*, 4850–4862.
- Morel, A., & Prieur, L. (1977). Analysis of variations in ocean color. *Limnology and Oceanography*, *22*, 709–722.

- Mueller, J. L., & Fargion, G. S. (2001). Ocean optics protocols for satellite ocean color sensor validation, revision, 3. In J. L. Mueller, & G. S. Fargion (Eds.), *NASA/TM-2002-210004*. Greenbelt, Maryland: Goddard Space Flight Centre.
- Nelson, J. R., & Robertson, C. Y. (1993). Detrital spectral absorption: Laboratory studies of visible light effects on phytodetritus absorption, bacterial spectral signal, and comparison to field measurements. *Journal of Marine Research*, 51, 181–207.
- O'Reilly, J., Maritorena, S., Mitchell, B. G., Siegel, D., Carder, K. L., Garver, S., Kahru, M., & McClain, C. (1998). Ocean color chlorophyll algorithms for SeaWiFS. *Journal of Geophysical Research*, 103, 24937–24953.
- Platt, T., & Sathyendranath, S. (1988). Oceanic primary production: Estimation by remote sensing at local and regional scales. *Science*, 241, 1613–1620.
- Pope, R., & Fry, E. (1997). Absorption spectrum (380–700 nm) of pure waters: II. Integrating cavity measurements. *Applied Optics*, 36, 8710–8723.
- Reynolds, R. A., Stramski, D., & Mitchell, B. G. (2001). A chlorophyll-dependent semianalytical reflectance model derived from field measurements of absorption and backscattering coefficients within the Southern Ocean. *Journal of Geophysical Research*, 106, 7125–7138.
- Roesler, C. S., & Perry, M. J. (1995). In situ phytoplankton absorption, fluorescence emission, and particulate backscattering spectra determined from reflectance. *Journal of Geophysical Research*, 100, 13279–13294.
- Roesler, C. S., Perry, M. J., & Carder, K. L. (1989). Modeling in situ phytoplankton absorption from total absorption spectra in productive inland marine waters. *Limnology and Oceanography*, 34, 1510–1523.
- Sathyendranath, S., Lazzara, L., & Prieur, L. (1987). Variations in the spectral values of specific absorption of phytoplankton. *Limnology and Oceanography*, 32, 403–415.